

Solid-State Transformations of Zinc 1,4-Benzenedicarboxylates Mediated by Hydrogen-Bond-Forming Molecules

Mark Edgar, Robert Mitchell, Alexandra M. Z. Slawin, Philip Lightfoot, and Paul A. Wright*^[a]

Abstract: The zinc 1,4-benzenedicarboxylates $[\text{Zn}_3(\text{bdc})_3(\text{H}_2\text{O})_3] \cdot 4\text{DMF}$ (**1**; bdc = 1,4-benzenedicarboxylate), $[\text{Zn}(\text{bdc})(\text{H}_2\text{O})] \cdot \text{DMF}$ (**2**), and $[\text{Zn}(\text{bdc})] \cdot \text{DMF}$ (**3**) crystallise at room temperature from mixtures of toluene/dimethylformamide (DMF) under concentrated, dilute and dry conditions, respectively. The structure of phase **1** (monoclinic: $P2_1/c$, $a = 13.065(1)$, $b = 9.661(1)$, $c = 18.456(1)$ Å, $\beta = 106.868(2)^\circ$) consists of layers containing stacks of three zinc cations linked by mono- and bidentate bdc groups. Structure **1** converts to the known phase **2** by an irreversible, reconstructive phase transformation, whereas **2** and **3** interconvert reversibly

upon the loss or addition of water. Removal of all solvent molecules included during crystallisation gives poorly crystalline $[\text{Zn}(\text{bdc})]$ (**4**), which is readily converted to highly crystalline solids upon contact with hydrogen-bond-forming molecules such as water, DMF and small alcohols. The crystal structures of the mono- and dihydrates $[\text{Zn}(\text{bdc})(\text{H}_2\text{O})]$ (**6**) and $[\text{Zn}(\text{bdc})(\text{H}_2\text{O})_2]$ (**7**) have been determined ab initio from powder X-ray diffraction

data (compound **6**, monoclinic: $C2/c$, $a = 17.979(1)$, $b = 6.352(1)$, $c = 7.257(1)$ Å, $\beta = 91.477(1)^\circ$; compound **7**, monoclinic: $C2/c$, $a = 14.992(1)$, $b = 5.0303(2)$, $c = 12.098(1)$ Å, $\beta = 103.82(1)^\circ$). The methanol adduct $[\text{Zn}_3(\text{bdc})_3] \cdot 6\text{CH}_3\text{OH}$ (**5**) is the same as that prepared previously by direct crystallisation. Comparison of these adduct structures with those prepared directly reveal that they are formed by in situ recrystallisations. Subsequent removal of included molecules gives amorphous $[\text{Zn}(\text{bdc})]$, which can be recrystallised again when placed in contact with hydrogen-bond-forming molecules.

Keywords: carboxylate ligands • inclusion compounds • organic–inorganic hybrid composites • structure elucidation • zinc

Introduction

There is currently great interest in the synthesis of porous organic–inorganic hybrid frameworks, as the chemistry of their internal surfaces differs markedly from that of inorganic solids such as microporous aluminosilicates or aluminophosphates.^[1] In principle, it is possible to imagine a wide range of different organic groups being used to make up the pore walls. These solids would be expected to display distinctive adsorption and separation behaviour. Organic–inorganic hybrid solids such as aluminium and other metal phosphonates, in which the organic moieties (methyl and aryl groups) line the internal surfaces, possess encouraging thermal stabilities in the absence of oxygen, and retain their crystallinity and porous structure upon loss of molecules included upon crystallisation.^[1] For metal–organic frameworks,^[2] in which

metal centres are linked by doubly or triply coordinating bridging ligands (such as diamines^[3] or di^[4] or tricarboxylates^[5]) the thermal stability is lower, and this aspect of their properties requires particular attention.

Zinc carboxylates have been shown to crystallise with a range of two- and three-dimensionally connected lattices.^[4, 5] Zinc benzenetricarboxylates^[6] have been shown to form well defined and structurally stable three-dimensional frameworks. It has been shown that adsorption of H_2O and NH_3 was possible for the desolvated $[\text{Zn}(\text{bdc})]$ but significant structural rearrangement took place for the cobalt and nickel forms,^[5c] indicating an inclusion process rather than adsorption.

Zinc benzenedicarboxylates^[7] crystallise at room temperature when bases such as amines are added to solutions that contain zinc salts and benzenedicarboxylic acids. The solvent mixes that have been employed include molecules that form strong hydrogen bonds such as dimethylformamide (DMF), methanol and thiourea.^[8] For thiourea adducts the resulting metal–carboxylates may occur as clusters, chains or sheets, depending on the isomer of the dicarboxylic acid used. Zinc benzenedicarboxylates crystallise in the presence of DMF and

[a] Dr. P. A. Wright, Dr. M. Edgar, R. Mitchell, Dr. A. M. Z. Slawin, Dr. P. Lightfoot
School of Chemistry, The University of St Andrews
St Andrews, Fife, KY16 9ST (UK)
Fax: (+44) 1334-463808
E-mail: paw2@st-and.ac.uk

methanol to form the two-dimensional lattice structures $[\text{Zn}(\text{bdc})(\text{H}_2\text{O})] \cdot \text{DMF}^{[9]}$ and $[\text{Zn}_3(\text{bdc})_3] \cdot 6\text{CH}_3\text{OH}$,^[10] respectively. The former is reported to give a solid that adsorbs small molecules from the vapour phase, whereas the latter is found to show reversible desorption and adsorption of some of the included methanol molecules.

As part of a research program to investigate the sorption behaviour of porous organic–inorganic hybrids, we have examined the structural changes associated with the loss and subsequent uptake of small volatile molecules capable of forming strong hydrogen bonds in zinc 1,4-benzenedicarboxylate solids. The latter are found to be reactive solids, which upon uptake of hydrogen-bond-forming molecules undergo structural changes typical of inclusion compounds rather than exhibiting the adsorption behaviour within fixed frameworks that is observed for conventional molecular sieves.

Results and Discussion

Direct crystallisation of zinc 1,4-benzenedicarboxylate hybrid materials:

The procedure of Yaghi^[9] was followed in an attempt to prepare $[\text{Zn}(\text{bdc})(\text{H}_2\text{O})] \cdot \text{DMF}$ (**2**) for subsequent study. Direct crystallisation from toluene/DMF solution was found to give $[\text{Zn}_3(\text{bdc})_3(\text{H}_2\text{O})_3] \cdot 4\text{DMF}$ (**1**), $[\text{Zn}(\text{bdc})(\text{H}_2\text{O})] \cdot \text{DMF}$ (**2**) or $[\text{Zn}(\text{bdc})] \cdot \text{DMF}$ (**3**) depending on the reaction conditions. To determine the conditions under which each solid might be formed directly, a flow experiment was devised in which a nitrogen-gas stream, saturated in triethylamine vapour, was permitted to bubble through or over the surface of the Zn/bdc solution. The crystals that formed after a few hours were determined to be compound **1** (Figures 1 and 2, top). A second crop of crystals was taken from the filtrate after 14 days and single-crystal and powder X-ray diffraction analyses indicated that they were compound **2** (Figures 3 and 2, bottom). Compound **3** was prepared from mixtures of dry solvents. The behaviour of compounds **1** and **2** was examined by thermogravimetric analysis (TGA), X-ray powder diffraction and solid-state NMR spectroscopy.

Compound **1** is a two-dimensional layered structure, with three zinc atoms forming a “stack” that is connected through a framework of bidentate and monodentate benzenedicarboxylates. The three-zinc-atom “stack” contains an octahedral zinc sandwiched between two tetrahedral zinc atoms ($Zn_{\text{oct}} - Zn_{\text{tet}} = 3.252(2) \text{ \AA}$), with the tetrahedrally coordinated zinc atoms binding to a terminal water ligand. Crystallographically distinct DMF molecules separate the $[\text{Zn}(\text{bdc})]$ layers and these molecules display $O_{\text{water}} - O_{\text{DMF}}$ distances of $2.614(7) \text{ \AA}$ that are typical of H-bonds.

Solid-state transformations on loss of included solvents:

Compound **1** was found to transform to compound **2** with loss of one DMF molecule per unit formula, upon standing in air over a period of days to weeks depending on the crystal quality and the storage conditions. The transformation can be readily followed in the bulk of the sample by X-ray powder diffraction (Figure 4, top) and in single crystals, by using crossed polarisation under the optical microscope. A reaction front can be seen to move rapidly through a crystal of **1** with

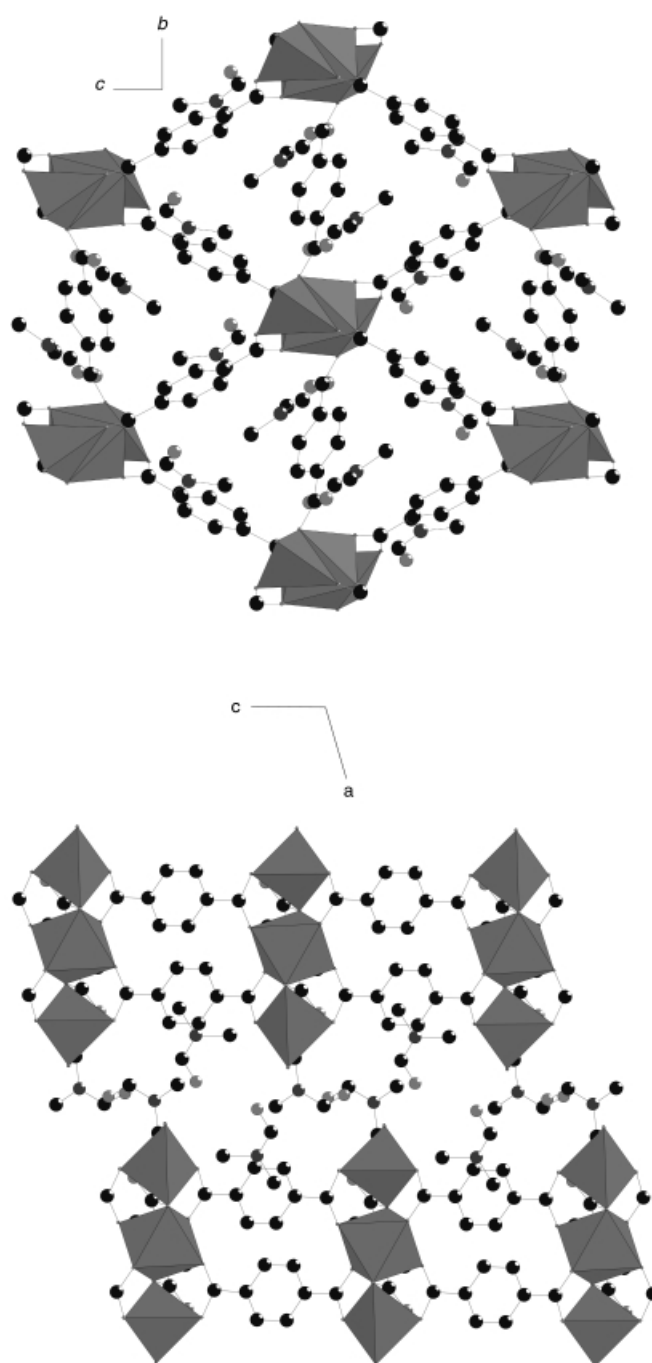


Figure 1. Structure of **1** from single-crystal data. Top: Viewed along the *a* axis through the lamellae, showing that DMF molecules appear to fill voids created by the framework. Bottom: Viewed along the *b* axis along the lamella, showing DMF molecules forming a hydrogen-bonded layer between the $[\text{Zn}(\text{bdc})]$ framework lamellae.

attendant loss of birefringence, indicating the transformation is not topotactic (Figure 5). The rate of interconversion was not accurately determined, but was observed to be related to crystal quality, with poorly formed crystals converting within a few hours and larger single crystals remaining stable for many days. Once initiated, the conversion process occurs within minutes. There is no evidence to support a drying-out process, which would be evident by a change in the outer surface of each crystallite. Comparison of the crystal structures (Fig-

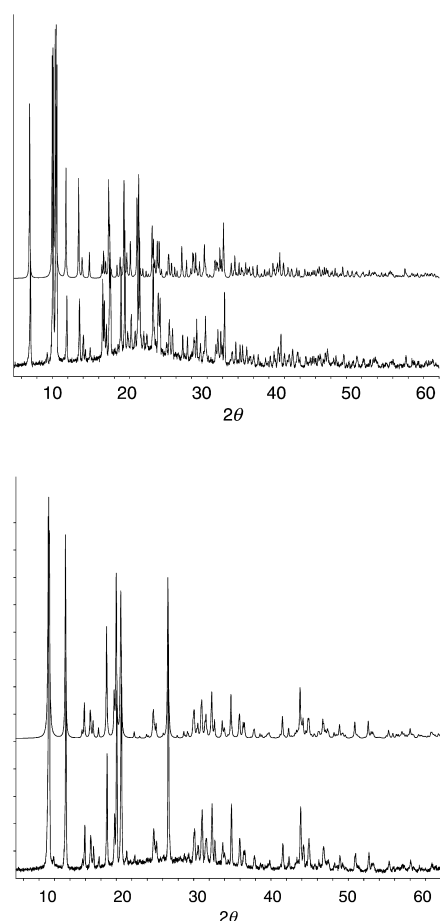


Figure 2. Top: Calculated (upper trace) and experimental X-ray powder diffraction pattern of **1**. Bottom: Calculated (upper trace) and experimental X-ray powder diffraction pattern of **2**.

ures **1** and **3**) confirms that the transformation is not topotactic. The layered structures are quite different, for example, in the precursor structure each “layer” contains units of three zinc polyhedra, whereas upon loss of DMF, the layers in compound **2** possess units of two pentahedrally coordinated zinc atoms ($Zn_{\text{pent}} - Zn_{\text{pent}} = 2.94 \text{ \AA}$). The layers are interdigitated with terminal water ligands from one layer protruding into voids of the neighbouring layer; each DMF molecule is arranged such that oxygen–oxygen distances, typical of hydrogen bonds, are present ($O_{\text{water}} - O_{\text{DMF}} = 2.60 \text{ \AA}$, $O-H-O = 172.4^\circ$).

Thermogravimetric analysis of the **2** indicates that solvent molecules are lost in two discrete events: between $65^\circ\text{C} - 115^\circ\text{C}$, 5.39 wt %, and $120 - 220^\circ\text{C}$, 21.48 wt %. The X-ray diffraction patterns of samples, heated to 90°C and 190°C to isolate the resulting solids, show that crystallinity is retained, but reduced (Figure 4, middle). ^{13}C $\{^1\text{H}\}$ CP-MAS NMR spectroscopy (Figure 6) indicated that DMF is retained in the intermediate solid (90°C), but is absent from the sample heated to 190°C , and analysis of the mass losses is consistent with water and DMF being lost in separate events.

As an aside, it has been shown that it is possible to form compound **3** directly by crystallisation from solution by using an almost identical experimental preparation as described above, with the additional precaution to ensure that all

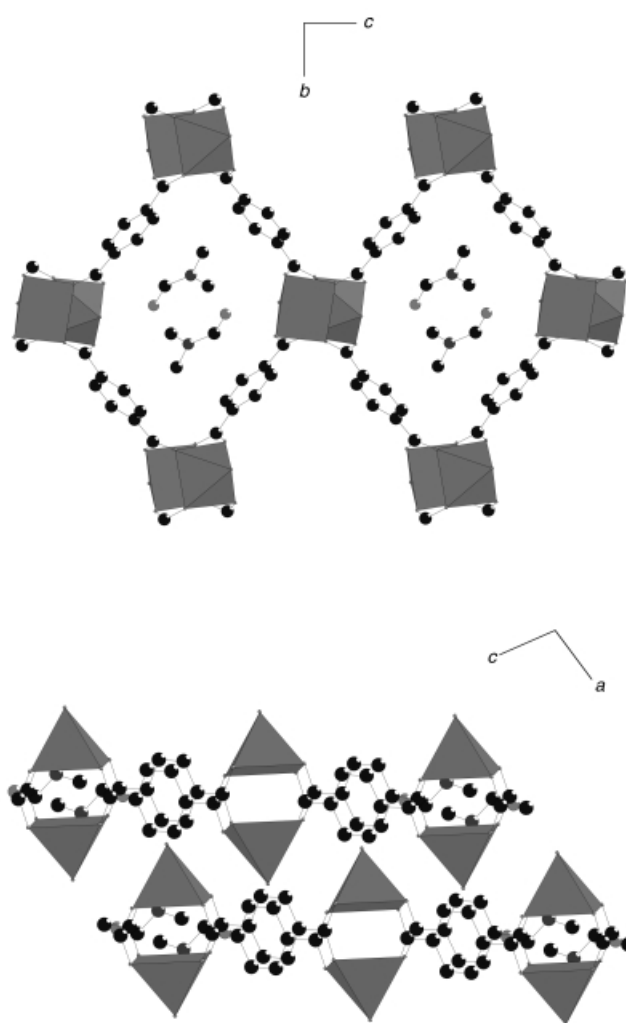


Figure 3. Structure of **2** from single-crystal data. Top: Viewed along the *a* axis through the lamellae, showing that DMF molecules appears to fill voids created by the framework. Bottom: Viewed along the *b* axis along the lamellae, showing hydrogen-bonded DMF molecules forming an integral part of the framework.

solvents are thoroughly dried prior to use (Figure 4c). Dry solvents readily yield crystalline **3** (triclinic: $a = 9.055(12)$, $b = 8.921(16)$, $c = 7.940(13) \text{ \AA}$, $\alpha = 99.90(8)^\circ$, $\beta = 100.91(6)^\circ$, $\gamma = 103.28(8)^\circ$) as determined by powder X-ray diffraction. These crystals undergo a solid-state recrystallisation and convert to compound **2** on exposure to air for several weeks as determined by X-ray powder diffraction.

Recrystallisation of the solvent-free solid upon exposure to hydrogen-bond-forming molecules—an examination of the reversibility of these transformations:

It was not possible to determine the structure of the sample produced by the loss of the solvent molecules included upon crystallisation, but it was chosen as a starting point for adsorption studies. Although a similar material, prepared by heating a sample of compound **2** that had been prepared directly from solution, was reported to possess microporosity ($270 \text{ m}^2 \text{ g}^{-1}$ with micropore volume of $0.11 \text{ cm}^3 \text{ mL}^{-1}$ ($0.094 \text{ cm}^3 \text{ g}^{-1}$)),^[9] our material showed no Type I adsorption of N_2 at 77 K. This significant difference between the physical properties of the two materials (they

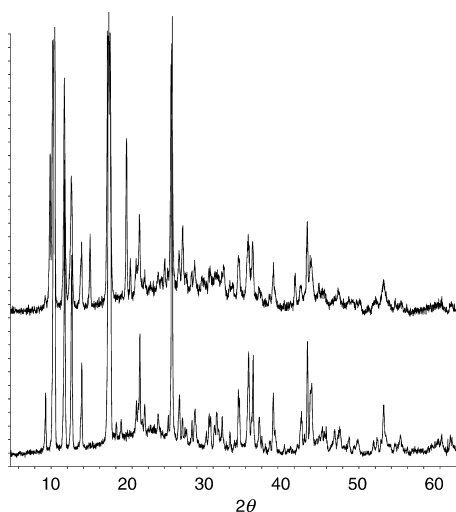
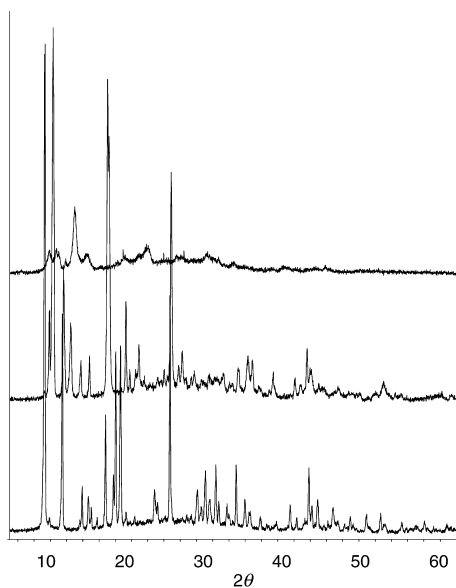
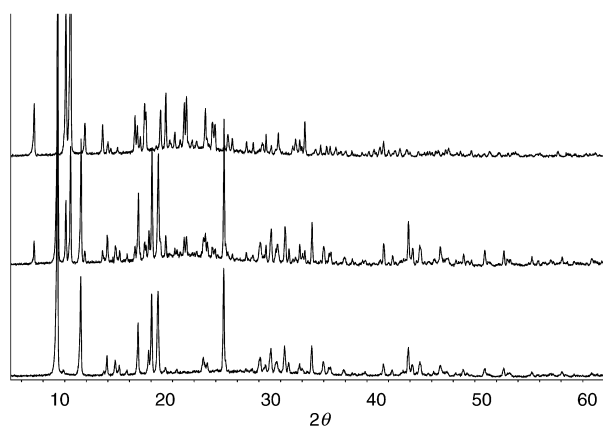


Figure 4. Top: Conversion of **1** (upper trace) to **2** (lower trace) on loss of DMF at room temperature over a period of 31 hours monitored using X-ray powder diffraction. The intermediate conversion (middle trace) was taken after 24 hours. Middle: Desolvation of **2** monitored using in situ variable temperature X-ray powder diffraction (lower trace 30 °C, middle trace 90 °C, upper trace 190 °C). The sample was loaded in an open ended 0.5 mm external diameter quartz capillary and heated in a furnace in 1 hour steps of 20 °C from 30 °C to 210 °C. Bottom: Comparison of **3** directly crystallised from solution (lower trace) with **3** formed by dehydration of **2** at 90 °C (upper trace).

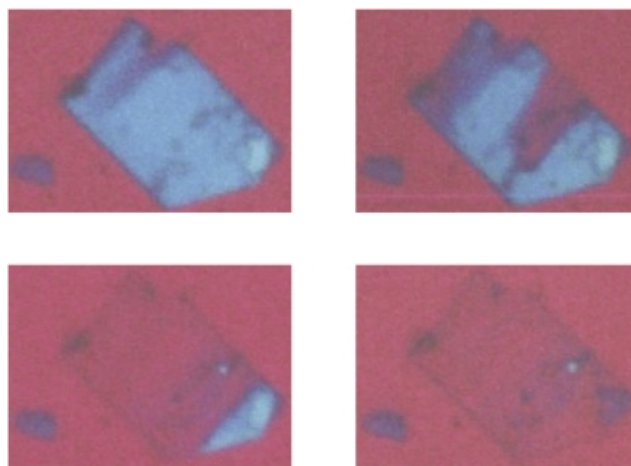


Figure 5. Optical microscopy (under crossed-polars) showing the temporal evolution of freshly prepared **1** on conversion to **2** on loss of a single DMF molecule.

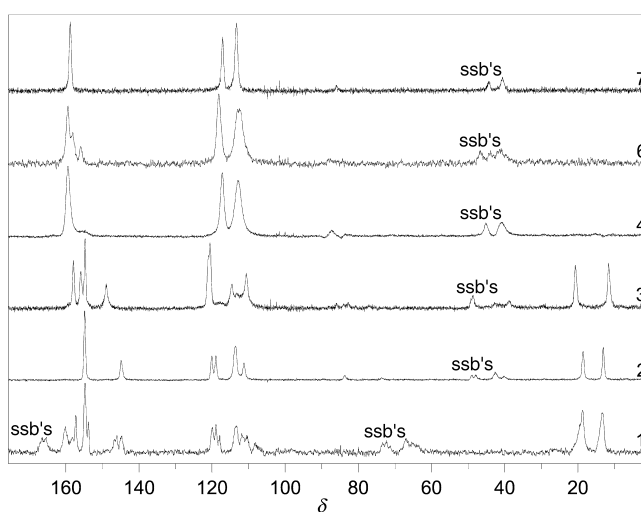


Figure 6. ¹³C CP-MAS NMR spectra of compounds **1–7** (“ssb’s” indicate spinning side bands).

have identical cell parameters) might be attributed to the microcrystalline nature of the starting material presented here. Also, our own N₂ adsorption measurements on large single crystals of directly synthesised **2** heated in vacuum at 120 °C (and 140 °C) gave no evidence for a Type I isotherm. Compound **2** can be described as an inclusion compound, with water and DMF molecules providing critical hydrogen bonds as well as acting as spacers. These results suggest that the [Zn(bdc)] structure is strongly rearranged, readily losing microporosity upon removal of solvent molecules.

Upon first exposing the [Zn(bdc)] (**4**; solvent-free) solid (prepared from both single crystals and from polycrystalline sample) to moist air and subsequently to DMF, it was possible to fully restore solid compound **2**, (in contrast to the reported behaviour of this solid).^[9] Exposure of the freshly desolvated **4** to a range of small molecules that exhibit strong hydrogen bonding, resulted in a series of highly crystalline solids. The samples prepared by exposure to methanol gave a powder pattern essentially identical to that reported by Yaghi^[10] for directly synthesised [Zn₃(bdc)₃]·6CH₃OH (**5**), with identical cell parameters. Examination of the structure of **5** indicated

that the layers contain units of three zinc polyhedra, with the zinc units linked by dicarboxylate ligands. Methanol acts as an interconnecting ligand between the zinc centres and also as an individual terminal ligand. There is, therefore, considerable structural rearrangement upon the transformation from compound **2** via **4** to compound **5**. Methanol is an integral component of this structure and not a guest molecule within a pore defined by a stable fixed framework.

The role of the included solvent in the framework structure is demonstrated by allowing the solid to lose methanol and take up water in moist air. This results in a solid-state recrystallisation and the formation of a highly crystalline monohydrate $[\text{Zn}(\text{bdc})(\text{H}_2\text{O})]$ (**6**). This material can be dehydrated to form **4**, which can then be treated with methanol to form compound **5**; this in turn can reform the monohydrate on loss of methanol. This interconversion loop between compounds **4**, **5** and **6** has been repeated up to five times without loss of crystallinity. The structure of this monohydrate was solved from the powder X-ray diffraction data (Figure 7, bottom) and was shown to consist of “zig-zag” chains of zinc–bdc units (Figure 7). All zinc centres exhibit trigonal bipyramidal coordination; monodentate bdc units and a bound water account for the trigonal arrangement, with longer Zn–O bonds to C=O functional groups of neighbouring chains binding the structure together ($\text{Zn}-\text{O}_{\text{bdc}} = 2.01$, $\text{Zn}-\text{O}_{\text{water}} = 1.99$, $\text{Zn}-\text{O}_{\text{C=O}} = 2.25$ Å). There is hydrogen bonding between the water molecule and the neighbouring chains, and zinc–oxygen bonds link one chain to two neighbouring ones. The structural integrity is insufficient to allow removal of the water without collapse of the framework. The monohydrate solid is a rather compact and dense structure without micropores. Dehydration of the monohydrate induced collapse of the “zig-zag” chain structure to yield amorphous **4**, which displayed no microporosity.

Upon addition of water to the fully desolvated **4**, or addition of water to the monohydrate, a highly crystalline dihydrate solid, $[\text{Zn}(\text{bdc})(\text{H}_2\text{O})_2]$ (**7**), forms, the structure of which was also determined from powder X-ray diffraction data (Figure 8, bottom). The structure is shown to consist of chains of distorted tetrahedral zinc centres linked through monodentate bdc groups to produce a “zig-zag” arrangement (Figure 8). The remaining two coordination sites around each zinc centre are occupied by water ligands that serve to provide hydrogen bonds within arrays of stacked chains and across to neighbouring chains. The distorted tetrahedra have typical bond lengths of $\text{Zn}-\text{O}_{\text{bdc}} = 2.01$ Å, $\text{Zn}-\text{O}_{\text{water}} = 2.02$ Å, with the hydrogen bonds within each stack of chains and between stacks of chains displaying O–O distances of 2.74 Å and 2.71 Å, respectively. The arrangement of the chains and the coordination of the zinc in the dihydrate solid is such that a three-dimensional network is not possible. If either the monohydrate or dihydrate again comes into contact with methanol, at room temperature, the methanol does not displace the water molecules from the structure. This material, unlike the monohydrate, cannot be readily dehydrated and reformed on contact with water for a second time (Scheme 1).

Similar behaviour to that observed upon addition of methanol is also seen if ethanol or 2-*tert*-butylphenol are

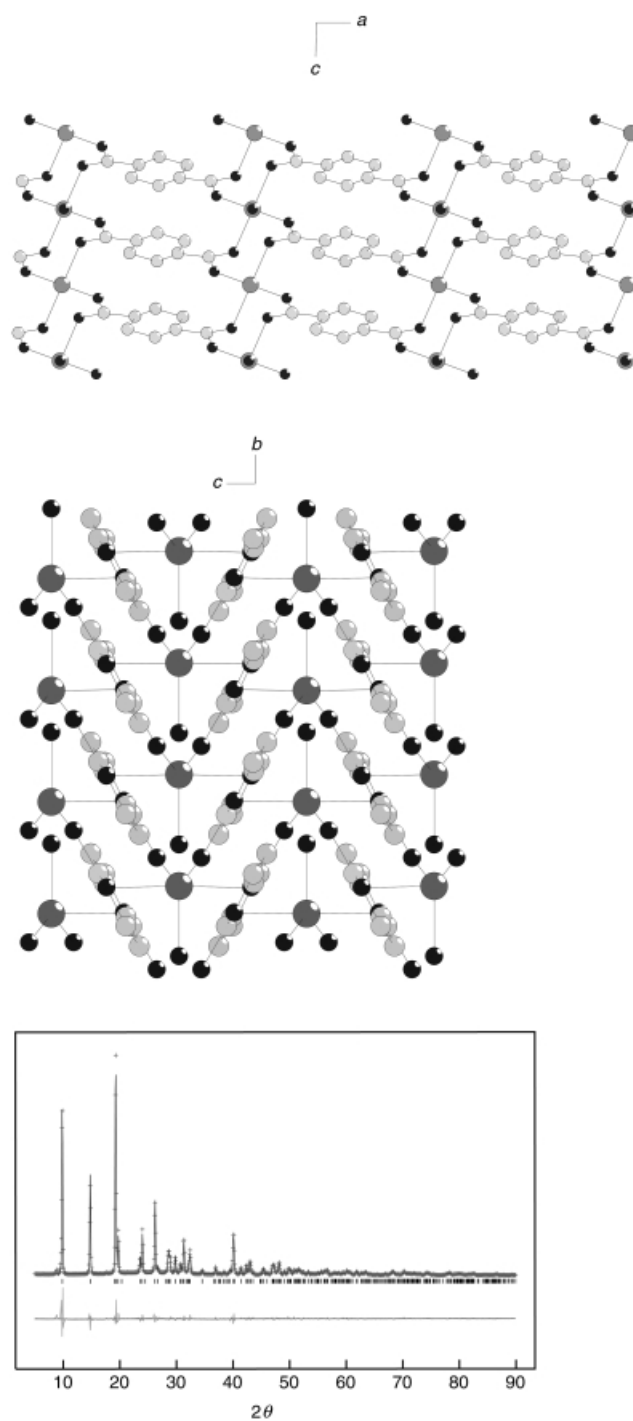


Figure 7. Structure of **6**. Top: Viewed along the *b* axis, highlighting the three-dimensional interconnected network. Middle: Viewed along the *a* axis, highlighting the “zig-zag” arrangement of the chains. Bottom: Final Rietveld refinement for **6**.

added to desolvated intermediate **4**. In each case recrystallisation to a new phase is followed, upon standing in moist air, by replacement of the alcohol by water to give the monohydrate. 2-*tert*-Butylphenol is a comparatively large molecule compared to any micropores available within the framework and would be expected to be excluded if the framework remained unchanged. However, it is the hydrogen-bonding ability of the solvent that is key in the recrystallisation and

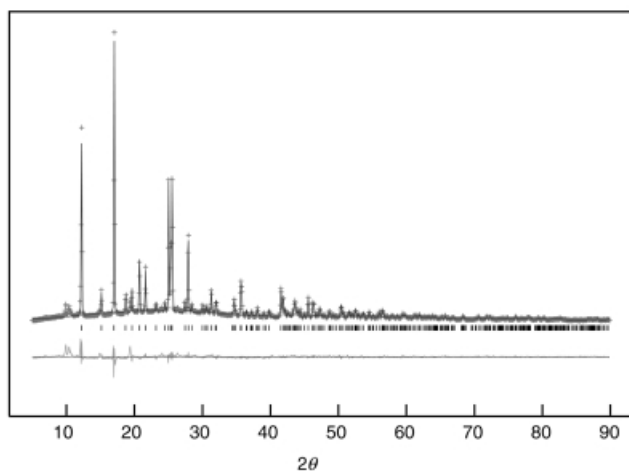
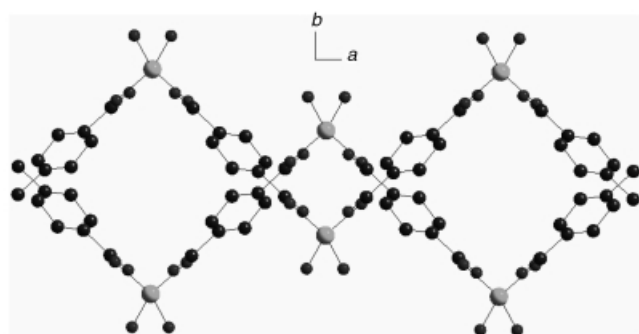
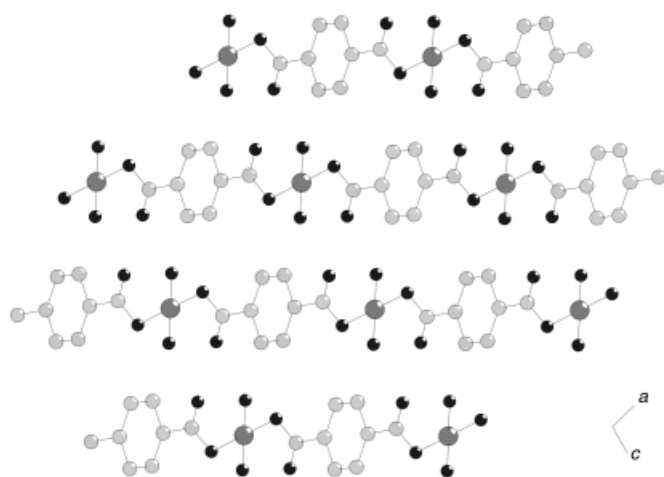
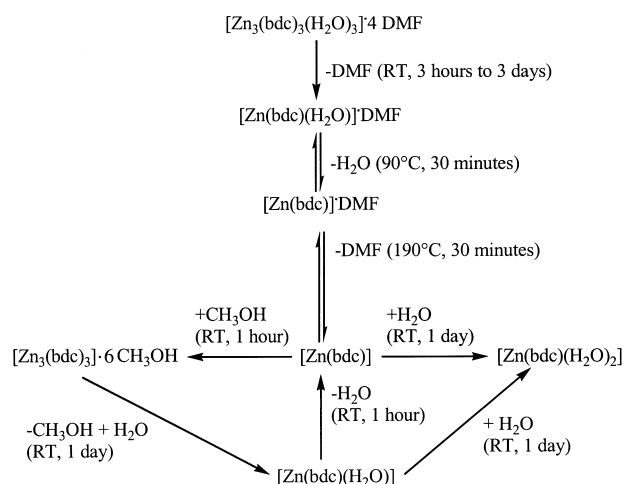


Figure 8. Structure of **7**. Top: Viewed along the *b* axis, highlighting the “chain-like” nature. Middle: Viewed along the *c* axis, highlighting the “zig-zag” arrangement of the chains. Bottom: Final Rietveld refinement for **7**.

subsequent formation of the monohydrate, and not the presence (or absence) of micropores.

Taken as a series, the increase in density of the zinc 1,4-benzenedicarboxylates on going from as-prepared **1** (1.515 g cm⁻³), **2** (1.678 g cm⁻³), **3** (1.679 g cm⁻³), **4** (unknown), **5** (1.731 g cm⁻³), **6** (1.936 g cm⁻³) to **7** (1.930 g cm⁻³) is illustrative of reconstructive changes of the structure, as hydrogen-bonding molecules are first lost and then subsequently taken up, rather than of a fixed framework with variable guest content.



Scheme 1. Reaction scheme summarising the chemistry of zinc benzenedicarboxylate.

A similar type of behaviour to that observed for these Zn(bdc) compounds, that is, the loss of crystallinity upon solvent removal followed by recrystallisation in the presence of hydrogen-bond-forming molecules, has been observed by Kepert et al. for a series of nickel 1,3,5-benzenetricarboxylates in the presence of alcohols.^[5c] They conclude on the basis of NMR and IR spectroscopy, that the poorly crystalline intermediate possessed a porous framework that readily re-adsorbed alcohols.

Solid-state ¹³C NMR spectra of the series of zinc 1,4-dicarboxylates studied in this work show the loss of DMF and the changes in environment of the carboxylate units. In particular, the spectra are consistent with compound **2** possessing only bidentate carboxylate units, whereas the chemical shift of intermediate **4** is closer to that observed for the dihydrate, in which the carboxylate unit is monodentate.

Conclusion

These studies indicate that the zinc dicarboxylates which are prepared by crystallisation at room temperature are highly reactive. Removal and replacement of strongly hydrogen-bonding molecules (DMF, methanol, ethanol, water) result in solid-state, reconstructive transformations, which can be considered as being mediated in situ by these “solvent” molecules. Observation of one such transformation under the optical microscope reveals a reaction front moving through a single crystal, and leaves a polycrystalline “pseudomorph”. Careful examination of the crystal structures of the reactant and product show that there are no common structural features, and there must be considerable structural rearrangement.

The [Zn(bdc)] that is prepared by removal of all DMF and water from the transformation product of compound **1** was not found to adsorb N₂. The difference between this solid and that reported by Yaghi may lie in pore blockage resulting from the polycrystalline nature of compound **2**, formed from the highly crystalline precursor **1**. Also, directly-synthesised large

(0.1 mm) single crystals of **2** did not give Type I adsorption behaviour when fully desolvated. The fully desolvated zinc 1,4-benzenedicarboxylate (**4**) was found to be highly reactive, and to take up DMF and water to reconstitute the original crystal structure of **2**. Furthermore, the desolvated solid recrystallised when placed in contact with small alcohols and water, giving highly crystalline solids, including compound **5**, which had previously only been prepared by direct crystallisation.

Our experiments show that suitable solvents enable the [Zn(bdc)] framework to connect in a variety of different forms; however, the structural integrity of the frameworks was not sufficient to enable removal of the solvent without concurrent recrystallisation or collapse of the framework. Subsequent inclusion of solvent molecules can be highly selective, and should be considered in light of framework formation rather than inclusion into a pre-existing framework.

Experimental Section

[Zn₃(bdc)₃(H₂O)₃]·4DMF (1**):** Triethylamine was allowed to come into contact, through vapour diffusion, with a solution of zinc nitrate (Zn(NO₃)₂·6H₂O, 0.95 g, 5.0 mmol), and benzene dicarboxylic acid (0.41 g, 2.5 mmol) in a mixture of toluene (70 mL) and dimethylformamide (35 mL). Solid crystalline material formed at the air–solvent interface within hours (typically 24 hours was required to provide sufficient yield), which was filtered and washed with toluene. Solid-state ¹³C NMR (125 MHz, 25 °C, adamantane): δ = 13.6 and 18.5 (CH₃)₂NCHO, 144 and 146 (CH₃)₂NCHO, 113.2–120.0 (bdc aromatic), 153.8–154.7 (bdc carbonyl).

[Zn(bdc)(H₂O)]·DMF (2**):** Triethylamine was allowed to come into contact, through vapour diffusion, with a solution of zinc nitrate (Zn(NO₃)₂·6H₂O, 0.095 g, 0.5 mmol), and benzene dicarboxylic acid (0.041 g, 0.25 mmol) in a mixture of toluene (70 mL) and dimethylformamide (35 mL). Solid crystalline material formed at the air–solvent interface after five days; this was filtered and washed with toluene. Solid-state ¹³C NMR (125 MHz, 25 °C, adamantane): δ = 13.7 and 18.5 (CH₃)₂NCHO, 144.8 (CH₃)₂NCHO, 111.2–120.0 (bdc aromatic), 154.8 (bdc carbonyl).

[Zn(bdc)]DMF (3**):** The synthesis of this compound was identical to that of compound **1** with the added provision of using dry solvents. Solid-state ¹³C NMR (125 MHz, 25 °C, adamantane): δ = 11.6 and 20.6 (CH₃)₂NCHO, 148.9 (CH₃)₂NCHO, 110.5–120.5 (bdc aromatic), 154.7–158.8 (bdc carbonyl).

[Zn(bdc)] (4**):** Compound **4** was formed by heating compound **2** for three hours at 190 °C. Solid-state ¹³C NMR (125 MHz, 25 °C, adamantane): δ = 113.0–117.1 (bdc aromatic), 159.5 (bdc carbonyl).

[Zn₃(bdc)₃]·6CH₃OH (5**):** Compound **5** was formed from compound **4** by steeping the solid in methanol for three hours. This material can also be formed directly by crystallisation for solution at room temperature.^[10]

[Zn(bdc)(H₂O)] (6**):** Compound **6** was formed upon the loss of methanol (at room temperature) from compound **5**. Solid-state ¹³C NMR (125 MHz, 25 °C, adamantane): δ = 113.3–117.1 (bdc aromatic), 158.7 (bdc carbonyl); elemental analysis calcd (%) for C₈H₆O₅Zn (247.4): C 38.81, H 2.42; found: C

38.90 H 2.10; TGA: calcd weight loss = 18.00 amu; experimental weight loss = 18.33 amu.

[Zn(bdc)(H₂O)]₂ (7**):** Compound **7** was formed directly from compound **4** on addition of water, and from compound **6** on addition of water followed by drying in air. Solid-state ¹³C NMR (125 MHz, 25 °C, adamantane): δ = 112.53–118.1 (bdc aromatic), 156.0–159.4 (bdc carbonyl); elemental analysis calcd (%) for C₈H₈O₆Zn (265.4): C 36.18, H 3.02; found: C 36.26 H 2.70; TGA: calcd weight loss = 36.0 amu; experimental weight loss = 36.46 amu.

X-ray crystallography: The single-crystal X-ray diffraction intensities were collected over a half hemi-sphere at 293 K on a Bruker CCD diffractometer employing graphite monochromated MoK_α radiation (λ = 0.71073 Å). The structures were solved by using direct methods and refined by full-matrix least-squares on F² using SHELXTL program. High-resolution powder X-ray diffraction data were collected by using a STOE Stadi/p diffractometer in transmission mode, scanning 2θ between 5° and 90°, with monochromatic CuK_α radiation (curved germanium (111)) with λ = 1.54056 Å). Samples were mounted between two sheets of mylar foil. Diffractograms were indexed by using the Visser and Louer algorithms available within the STOE WINXPOW software. For ab initio structure solution, pattern decomposition using the Le Bail method^[11] was carried out over the range 5° < 2θ < 60°, with the GSAS suite.^[12] For both **6** and **7**, Zn positions were determined by Patterson methods by using SHELXS97.^[13] The remaining non-H atoms were located from difference Fourier maps derived from Rietveld refinement of the full powder diffraction profile. All non-H atoms were refined isotropically, with no restraints being required. H atoms were not located. Further details are given in Tables 1–6. Crystallographic data (excluding structure factors) for the structures reported in this paper have been deposited with the Cambridge Crystallographic Data Centre as supplementary publication no. CCDC-171974, CCDC-171975, CCDC-171952 and CCDC-171953. Copies of the data can be obtained free of charge on application to CCDC, 12 Union Road, Cambridge CB2 1EZ, UK (fax: (+44) 1223-336-033; e-mail: deposit@ccdc.cam.ac.uk).

Solid-state NMR spectroscopy: ¹³C {¹H} CP-MAS NMR spectra were recorded by using a Bruker MSL 500 MHz instrument with spinning speeds of up to 9.5 kHz, dipolar-dephasing filters of between 100 μs and 500 μs were employed at the beginning of the FID acquisition in order to assign aromatic C and CH groups, and dicarboxylate and DMF carbonyl groups. Processing was carried out with Bruker WINNMR software and spectra were fit and analysed with WINMAS and WINFIT.

Optical microscopy: The transformation of single crystals of **1** was followed under the optical microscope. Photographs were taken with a Kodak

Table 1. Single-crystal data for compounds **1**, **2** and **5**.^[10]

	1	2	5
crystal dimensions [mm]	0.11 × 0.1 × 0.01	0.12 × 0.1 × 0.01	
crystal system	monoclinic	monoclinic	triclinic
space group	<i>P</i> ₂ / <i>c</i>	<i>P</i> ₂ / <i>n</i>	<i>P</i> $\bar{1}$
<i>a</i> [Å]	13.065(1)	6.733(1)	9.726(4)
<i>b</i> [Å]	9.661(1)	15.516(1)	9.911(5)
<i>c</i> [Å]	18.456(1)	12.453(1)	10.450(5)
α [°]			99.72(4)
β [°]	106.87(1)	102.80(1)	111.11(4)
γ [°]			108.42(4)
<i>V</i> [Å ³]	2229.2(3)	1268.7(1)	844.9(7)
<i>Z</i>	2	4	2
ρ _{calcd} [Mg m ⁻³]	1.515	1.678	1.731
λ [Å]	0.71073	0.71073	0.71073
θ range [°]	1.63–23.27	2.13–23.25	2.20–25.05
<i>T</i> [K]	293 (2)	293 (2)	293 (2)
measured reflections	12 342	5472	3577
independent reflections	3204 (<i>R</i> _{int} = 0.0949)	1819 (<i>R</i> _{int} = 0.0538)	2998 (<i>R</i> _{int} = 0.0423)
refinement	full-matrix least-squares on <i>F</i> ²		
absorption correction/max/min	Sadabs/1.00000/0.560220	Sadabs/1.00000/0.789698	Psi scan/0.786/0.670
data/restraints/parameters	3154/2/286	1773/3/181	2998/0/236
<i>R</i> (obs)	0.0441	0.0347	0.0642
<i>R</i> _w (obs)	0.0944	0.0667	0.1395
<i>F</i> ² (goodness of fit)	0.873	1.035	1.024

Table 2. Powder X-ray data for compounds **3**, **6** and **7**.

	3 ^[a]	6	7
crystal system	triclinic	monoclinic	monoclinic
space group	$P\bar{1}$	$C2/c$	$C2/c$
a [Å]	9.055(1)	17.979(1)	14.992(8)
b [Å]	8.921(2)	6.353(3)	5.030(2)
c [Å]	7.940(1)	7.257(3)	12.098(5)
α [°]	99.90(8)		
β [°]	100.91(8)	91.47(4)	103.82(3)
γ [°]	103.28(8)		
V [Å ³]	597.5 (27)	828.6 (9)	886.0 (9)
Z	2	2	2
ρ_{calcd} [Mgm ⁻³]	1.679	1.936	1.930
λ [Å]	1.54056	1.54056	1.54056
2θ range [°]	5–60	5–90	5–90
T [K]	293	293	293
reflections used for solution	–	101	131
reflections used for refinement	–	353	397
total parameters	–	41	44
R_{wp}	–	0.1147	0.1146
χ^2	–	27.21	12.88

[a] Indexed from powder diffraction data collected from directly crystallised material.

Table 3. Fractional atomic coordinates for compound **6**.

	x	y	z	U_i ($\times 100$)
Zn1	0.000000	0.6863(6)	0.250000	2.29(1)
O2	–0.0982(5)	0.5659(17)	0.1599(14)	1.72(3)
O3	0.000000	1.0048(19)	0.250000	1.72(3)
O4	–0.0476(4)	0.7067(15)	0.5343(11)	1.72(3)
C5	–0.1126(7)	0.3875(23)	0.0668(23)	1.37(3)
C6	–0.1839(8)	0.2942(33)	0.0329(18)	1.37(3)
C7	–0.2410(1)	0.4592(21)	0.0904(20)	1.37(3)
C8	–0.1892(9)	0.1080(28)	–0.0538(21)	1.37(3)

Table 4. Selected bond lengths [Å] and bond angles [°] for compound **6**.

Zn1–O2	2.02(1)	Zn1–O3	2.02(1)	O2–Zn1	2.02(1)
O4–C5	1.34(1)	O2–O4	2.17(1)	O2–C5	1.34(1)
C6–C8	1.34(2)	C5–C6	1.43(2)	C6–C7	1.53(2)
C8–C7	1.34(3)	C7–C8	1.34(2)	C8–C6	1.34(2)
O2–Zn1–O2	135.5(6)	O2–Zn1–O3	112.3(3)	C5–C6–C8	119.9(2)
O2–Zn1–O4	88.2(4)	O2–Zn1–O4	94.3(3)	C6–C7–C8	110.9(1)
O3–Zn1–O4	86.7(3)	O4–Zn1–O4	173.4(6)	C5–C6–C7	105.9(2)
O4–O2–C5	129.7(2)	O2–O4–C5	119.2(2)	C7–C6–C8	133.6(2)
O2–C5–O4	108.0(1)	O2–C5–C6	126.7(2)	C6–C8–C7	115.3(2)
O4–C5–C6	124.6(2)				

Table 5. Fractional atomic coordinates for compound **7**.

	x	y	z	U_i ($\times 100$)
Zn1	0.500000	0.0643(7)	0.250000	4.18(2)
O2	0.5527(6)	–0.2134(16)	0.1620(8)	2.96(2)
O3	0.3944(7)	0.3271(17)	0.2121(8)	2.96(2)
C4	0.3094(11)	0.5809(28)	0.0464(14)	1.80(3)
O5	0.4378(7)	0.2617(16)	0.0496(8)	2.96(2)
C6	0.2407(13)	0.6237(28)	0.1063(11)	1.80(3)
C7	0.3241(10)	0.6778(30)	–0.0572(14)	1.80(3)
C8	0.3849(11)	0.3712(28)	0.1063(12)	1.80(3)

800 ASA colour film in a Centron DF-300 camera mounted on a Prior optical microscope employing crossed-polars and filter. The freshly prepared crystalline precursor material **1** displayed birefringence when viewed under crossed polars; this allowed the transformation to compound **2** to be monitored.

Table 6. Selected bond lengths [Å] and bond angles [°] for compound **7**.

Zn1–O2	2.03(1)	Zn1–O3	2.03(1)	C6–C7	1.42(2)
Zn1–C8	2.64(1)	O3–C8	1.27(1)	C4–C6	1.41(2)
C4–C7	1.41(2)	C4–C8	1.59(2)	O5–C8	1.29(1)
O2–Zn1–O2	92.9(5)	O2–Zn1–O3	135.3(3)	O3–C8–C4	118.1(1)
O2–Zn1–C8	100.8(4)	O3–Zn1–C8	98.7(5)	C4–C8–O5	120.1(2)
Zn1–O3–C8	103.6(9)	C6–C4–C7	133.8(2)	C4–C7–C6	112.2(1)
C6–C4–C8	113.3(2)	C7–C4–C8	112.9(2)	O3–C8–O5	121.7(1)
C4–C6–C7	113.8(1)				

Thermogravimetric analysis: The interconversion from **1** to **3** occurs through the loss of DMF from the crystal lattice. Thermo-gravimetric analysis (TGA) was performed between 30 °C and 600 °C under both nitrogen and oxygen gas flow, with a TA Instrument thermal balance and analysed by using TA Instrument Universal Analysis software.

Acknowledgement

The EPSRC are thanked (ME) for financial support, Humphrey Yiu for assistance with the TGA measurements, Sylvia Williamson for CHN analysis, and Milanja Smith and Frank Riddell for NMR expertise.

- [1] a) K. Maeda, A. Sasaki, K. Watanabe, Y. Kiyozumi, F. Mizukami, *Chem. Lett.* **1997**, 9, 879; b) K. Maeda, Y. Kiyozumi, F. Mizukami, *J. Phys. Chem. B* **1997**, 101, 4402; c) K. Maeda, J. Akimoto, Y. Kiyozumi, F. Mizukami, *J. Chem. Soc. Chem. Commun.* **1995**, 1033; d) V. J. Carter, P. A. Wright, J. D. Gale, R. E. Morris, E. Sastre, J. Perez-Pariente, *J. Mater. Chem.* **1997**, 7, 2287; e) G. Alberti, R. Vivani, F. Marmottini, P. Zappelli, *J. Porous Mater.* **1998**, 5, 205; f) A. Clearfield, D. Wang, Y. Tian, E. Stein, C. Bhardwaj, *J. Solid State Chem.* **1995**, 117, 275.
- [2] a) O. M. Yaghi, C. E. Davis, H. Li, D. Richardson, T. L. Groy, *Acc. Chem. Res.* **1998**, 31, 474; b) M. Eddaoudi, D. B. Moler, H. Li, B. Chen, T. M. Reineke, M. O'Keeffe, O. M. Yaghi, *Acc. Chem. Res.* **2001**, 34, 319.
- [3] a) C. J. Kepert, M. J. Rosseinsky, *Chem. Commun.* **1998**, 31; b) C. Livage, C. Egger, M. Noguez, G. Ferey, *J. Mater. Chem.* **1998**, 8, 2743; c) F. Serpaggi, G. Ferey, *Microporous Mesoporous Mater.* **1999**, 32, 311; d) O. M. Yaghi, H. L. Li, T. L. Groy, *Inorg. Chem.* **1997**, 36, 4292; e) S. Subramanian, M. J. Zaworotko, *Angew. Chem.* **1995**, 107, 2295; *Angew. Chem. Int. Ed. Engl.* **1995**, 34, 2127.
- [4] a) C. J. Kepert, T. J. Prior, M. J. Rosseinsky, *J. Solid State Chem.* **2000**, 152, 261; b) M. J. Plater, M. R. St J. Foreman, E. Coronado, C. J. Gomez-Garcia, A. M. Z. Slawin, *J. Chem. Soc. Dalton Trans.* **1999**, 4209.
- [5] a) T. M. Reineke, M. Eddaoudi, M. O'Keeffe, O. M. Yaghi, *Angew. Chem.* **1999**, 111, 2712; *Angew. Chem. Int. Ed.* **1999**, 38, 2590; b) T. M. Reineke, M. Eddaoudi, M. Fehr, D. Kelly, O. M. Yaghi, *J. Am. Chem. Soc.* **1999**, 121, 1651; c) C. J. Kepert, T. J. Prior, M. J. Rosseinsky, *J. Am. Chem. Soc.* **2000**, 122, 5158.
- [6] a) O. M. Yaghi, C. E. Davis, G. M. Li, H. L. Li, *J. Am. Chem. Soc.* **1997**, 119, 2861; b) O. M. Yaghi, C. E. Davis, G. M. Li, H. L. Li, *J. Am. Chem. Soc.* **1996**, 118, 9096; d) O. M. Yaghi, R. Jernigan, H. Li, C. E. Davis, T. L. Groy, *J. Chem. Soc. Dalton Trans.* **1997**, 2383.
- [7] H. Li, M. Eddaoudi, M. Keefe, O. M. Yaghi, *Nature* **1999**, 402, 276.
- [8] A. D. Burrows, R. W. Harrington, M. F. Mahon, C. E. Price, *Dalton* **2000**, 3845.
- [9] H. Li, M. Eddaoudi, T. L. Groy, O. M. Yaghi, *J. Am. Chem. Soc.* **1998**, 120, 8571.
- [10] H. L. Li, C. E. Davis, T. L. Groy, D. G. Kelley, O. M. Yaghi, *J. Am. Chem. Soc.* **1998**, 120, 2186.
- [11] A. Le Bail, *J. Solid State Chem.* **1989**, 83, 267.
- [12] A. Larson, R. Von Deele, Los Alamos National Laboratory, Report No. LA-UR-86–748, **1987**.
- [13] G. M. Sheldrick, SHELXTL, Program for the solution of crystal structures, University of Göttingen, **1993**.

Received: May 7, 2001 [F3243]